LTspice Model of a Solar Thermoelectric Generation System

Yacouba Moumouni and R. Jacob Baker
Department of Electrical and Computer Engineering, University of Nevada, Las Vegas
yacoubam@unlv.nevada.edu

Abstract—**Transient heat transfer analysis by means of analytical methods is known to be cumbersome. This paper seeks to develop an LTspice model of a real-world solar thermoelectric generation system. The thermal parameters of the proposed model were extracted from a multitude of parts' geometries and properties. These parameters were then converted into their electrical equivalences through the "*thermal-to-electrical analogy*." In addition, real site data were fed into the Spice model via the built-in piecewise linear command in order to implement the real system's thermal behavior. An interesting *RC* analogy was derived from this model in order to demonstrate how thermoelectric generation systems respond to square wave-like solar radiation. Although temperature variations on the cold side of this LTspice model are roughly 80% accurate, simulation results and the actual experiment remain in good agreement.**

Index Terms—**Internal parameter variation, LTspice, modeling and simulation, real-world experiment, renewable energy, solar thermoelectric generator**

I. Introduction

It is a well-known fact that energy is vital to the extent that it completes and sustains billions of luxurious lives today. Without energy, cold and hunger would leave many people vulnerable to all sorts of diseases. Fossil fuels are irrefutably the major source of energy across the World—80 to 85%, whereby the most dominants are oil, coal, and natural gas. Energy emanating from fossil fuel is somewhat less expensive to produce. In addition, most of the technology today is geared toward the utilization of remnant fuels. Nevertheless, the latter are non-regenerative energy sources at a human scale, and are destined to be depleted in the future. Some of the alternative sources, such as wind, hydropower, and geothermal destroy the environment on the long run.

Solar energy is one of the most abundant and cleanest renewable sources in the universe. It doesn't produce greenhouse gases (*GHG*) and other harmful environmental pollutants. It also requires no incursion upon the natural wild animals' habitats if harnessed with environmentally-friendly semiconductor devices, such as photovoltaic (*PV*) and thermoelectric generator (*TEG*). In fact, solar energy's immensity, year round availability, and benign effect on the climate, have made it the most appealing energy source on Earth. In spite of the versatility and abundance of solar energy, very little of it is directly utilized to power human activities. If solar energy were to become a concrete alternative to fossil fuels, efficient ways to convert photons into electricity and useful heat must be developed [1]. However, problems with solar renewable energy include variability due to weather events and its nocturnal absence [2]. Since solar energy is, most of the time, stochastic in nature, there is a great need for energy storage. It is worth pointing out that, energy storage can be utilized to mitigate renewable system transients[3].

Therefore, numerous experiments investigating TEG modeling through the thermal-to-electrical analogy schemes have been conducted [4]–[9]. Not all of these research works considered the effects of internal parameters' variation with temperature, such as the inductance and capacitance. A detailed method of how to extract these parasitic components can be found in [10]. A step-by-step method of analyzing transient heat transfer by means of the thermal-to-electrical analogy was detailed in our previous work [11]. Consequently, the steps it takes to simulate any thermo-electrical system with the electronic LTspice simulator are wittingly over-looked in the current paper.

This paper makes an attempt to model, with the LTspice simulator, a real-world environment solar thermoelectric generation system (*STEG*). The proposed model, which is comprised of five commercial Bismuth Telluride (Bi_2Te_3) TEGs, is based on the internal parameter fluctuations, such as Seebeck coefficient, parasitic inductance (*L*) and capacitance (*C*), and the internal resistance of the TEG. In addition, the STEG energy harvester was mounted on a dual-axis solar tracker. The thermal resistances and capacities of the entire STEG's physical parts were computed from device geometries and properties, and then converted into equivalent electrical quantities. The electrical quantities were then connected either in series and/or parallel to form the final circuit. Also, a novel *RC* analogy, solely applicable to any real-environment STEG energy harvesting system was investigated. It is important to specify that the values of the parasitic *C* and *L* were borrowed from a previous work reported in [10] because they cannot be determined with the equipment available to us.

II. Thermoelectric Generator Basic Principles

The concept of thermoelectricity came to existence after the discovery by the German Physicist, Thomas Seebeck, in 1821. He found that when two dissimilar metals form a circuit, with their junctions kept at different temperature, a compass magnet would be deflected, i.e., a thermo-electromotive force is generated, as seen in Fig. 1. Thus, thermoelectric generation is one of the various ways of converting electromagnetic energy into electrical energy through the Seebeck effect. Today, PN junction semiconductor devices, such as Bismuth

Telluride and its alloys have the biggest share on the market as they have proved to: 1) be reliable; 2) have no moving parts; 3) require no maintenance; and 4) are silent during their operation. The P and N type semiconductor devices that made up the TEG are connected electrically in series, but thermally attached in parallel between two ceramic substrates.

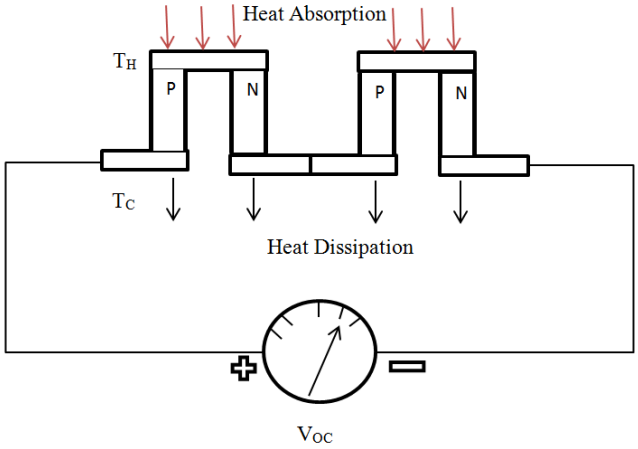

Figure 1 – Working theory of TEG system

Hence, the potential difference, V_{OC}, of the TEG is given by (1), as follows.

$$V_{OC} = n \cdot \alpha \cdot \Delta T. \quad (1)$$

In which, n, α, and ΔT are the number of cells (in this case n = 2), the Seebeck coefficient or the proportionality constant of the TEG, and ($T_H - T_C$) is the temperature differential, respectively.

III. Solar TEG System Modeling in LTspice

This work proposes to design, build, and test a solar thermoelectric generation system for energy delivery in remote residential areas. Possible methods to better understand its functionality and optimize its performance, i.e. the heat transfer capabilities between the top and the bottom surfaces, were investigated. The thermal-to-electrical analogy scheme was adopted to simulate the designed energy harvesting model by means of the LTspice simulator software. Experimental and simulated results were collected and then succinctly analyzed.

A. Extracted Parameters

Electrical parameters were extracted from datasheet and both device geometries and properties. A total of five TEGs were used in the proposed energy harvesting system. The modules were specified by the manufacturer to be bismuth telluride (Bi_2Te_3) and that the ceramic substrates were made of alumina (Al_2O_3). So, some of the properties that turned out to be useful in the succeeding computations were densities, specific heat capacities, and the thermal conductivities of the aluminum heat sinks, the substrate, and the Bi_2Te_3. The heat capacity and the internal thermal resistance of each module were estimated in the previous work to be 23 J/K and 0.64 K/W, respectively [11]. The former value was further split into two equal parts to fit in the LTspice model, as that yielded accurate STEG modeling and the best possible solutions. Also, the thermal resistance of the heat transfer grease, applied between the TEGs and the main heat sink, was assumed to be 0.45 $K.W$ [12]. Thus, without going into the details of calculations, the rest of the parameters necessary in performing the thermal-to-electrical analogy are concisely summarized in Table I. Besides, in computing the thermal resistance and capacitance of the physical parts, their various geometries and properties were solely taking into account.

TABLE I – LISTS OF THE EXTRACTED PARAMETERS

Designations	Thermal resistance (K/W)	Thermal capacitance (J/K)
TEG	0.64	23
Main heat sink	0.075	2694
Lateral sink	0.112	970
Insulation foam	109	91

B. System's Setup

The heat absorbing side of the TEGs was exposed to four reflectors covered with a highly reflective thin film material. These reflectors attached to a solar tracker, were positioned in such a way that the sun was concentrated four times on the devices. In addition, on top of the emitting side of the TEGs was sitting an aluminum heat exchanger which created the requisite differential temperature between the two sides. In order to prevent the four suns to shine directly on the heat exchanger, polyurethane insulation foam was glued around the set of TEGs. Also, a secondary heat sink was utilized to remove the heat from the bifacial solar flux sensor utilized to record the four suns. Stated clearly, the role of each one of these heat exchangers is independent from one another and they are of the extruded type, made of pure aluminum material. Therefore, only the former is given further consideration in this work as it played an essential role.

C. Electrical Analogy of Thermal System

So, modeling a thermoelectric module with LTspice would have been confusing, had it not been clearly explained methodically step-by-step in proceeding works. Therefore, the steps it takes to simulate any thermo-electrical system with the electronic LTspice simulator are over-looked in the current paper as the topic was already treated in detail [11].

D. Solar TEG Implementation in LTspice

The most important benefit of utilizing the LTspice simulator to model a complex transient heat transfer process is the convenience in viewing and interpreting the interactions between the four major effects: 1) *Seebeck*; 2) *Joule*; 3) *Peltier*; and 4) *Thomson*. Hence, voltage-dependent sources methodology is adopted in this work for rapid convergence purposes. This study did also incorporate the Seebeck coefficient, the thermal conductivity, and the internal thermal resistance variation with temperatures in the following LTspice model through the arbitrary behavioral voltage sources (*ABVS*). Conclusively, as can be seen in Fig. 2, all the parts obtained via the thermal-to-electrical analogies were either connected in series, and/or in parallel, to achieve the proposed solar TEG model.

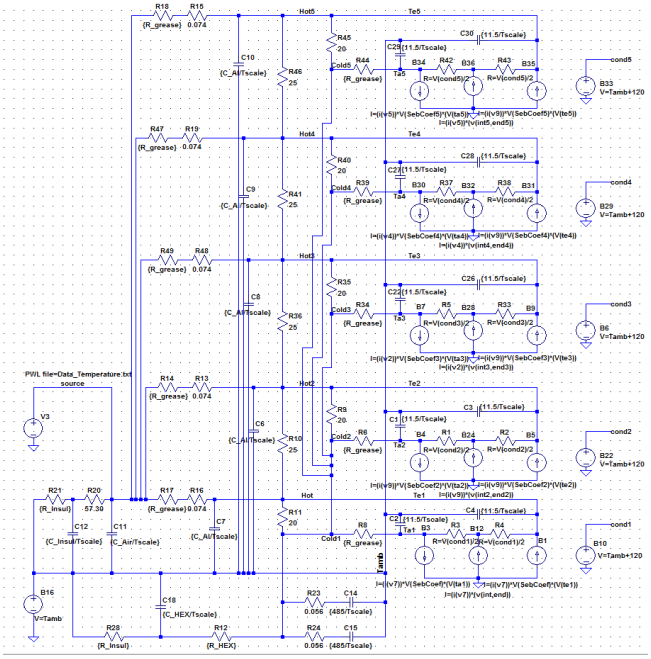

Figure 2 – Proposed thermal model of the STEG System

IV. An RC Analogy of a TEG

It has been proven throughout this research that the solar irradiance is directly proportional to the temperature on the hot side of the TEG set. So, an impulse of light was organized in a lookup table to simulate the local direct normal irradiance (*DNI*) and then fed into the Spice model via the built-in LTspice piece wise linear command. Hence, *V (Te2)*, denoting the temperature on the hot side of each one of the five TEGs as can be seen in Fig. 3, follows the exact same pattern of the impulse light. In the same figure, *V (Ta2)* denotes the temperature on the absorbing side. It is worth mentioning that two parameters, the internal parasitic capacitance (*C*) and the internal resistance (*R*) of the TEG, turned out to be of great importance in the current study. Fig. 3 illustrates a way of analyzing this behavior using an RC circuit. The impulse data were fed through V_3 (*low left of Fig. 2*).

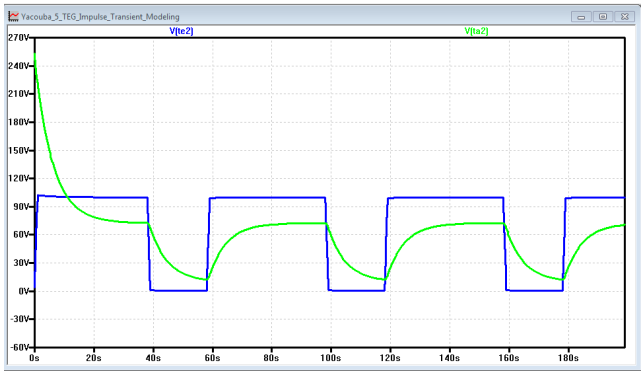

Figure 3 – Ramp rate in an STEG circuit

If the input square wave, which is temperature in this study, transitions from 0C to 100C (T_{pulse}), then the temperature across the cold side of the TEG is calculated as

$$T_{Cold}(t) = T_{pulse} \cdot \left(1 - (\mathrm{e})^{-\frac{t}{RC}}\right) + T_{Initial}\ . \qquad (2)$$

Where, T_{Cold}, T_{pulse}, and t are the temperature on the emitting side, temperature on the absorbing side, and the time variable, respectively; $T_{Initial}$ is assumed equal to zero.

Also, it should be mentioned that due to the internal parasitic components' effects, such as inductance and capacitance on one hand, and the effect of the heat sink on the other hand, the TEG RC analogy is slight different from the traditional RC circuit behavior. In essence, the Seebeck theory is only applicable if a certain temperature differential appears across the TEG. So, by virtue of that, when steady state is reached, T_{pulse} and T_{Cold} are quite alike. In addition to that, when the applied pulse goes to zero, *V (Ta2)* stays at certain threshold value because of the same aforementioned reasons.

In other words, the time it takes the TEG to reach half of the input pulse, although not similar to the conventional delay time, t_d, can be calculated by

$$\frac{T_{pulse}}{3} = T_{pulse} \cdot \left(1 - (\mathrm{e})^{-\frac{t}{RC}}\right) \Rightarrow t_d \approx 0.4 \cdot RC. \qquad (3)$$

The new *RC* theory has some limitations because it is only applicable to TEGs for now. T_{Cold}, as can be seen from Fig. 3, begins its ascension at 10% of the applied pulse. It flattens out at approximately 80% of the latter temperature, which implies that all the computations and the subsequent reasoning would be in the useful range of 0.6 to $0.7T_{pulse}$.

From conventional RC circuit theory, the rise time is known to be the time the output pulse takes to go from 10% to 90% of the input pulse. In this particular similitude, we are dealing with temperature rather than voltage. So, in the solar thermoelectric generation *RC* analogy, it goes from 20% to 60%, as can be seen in Fig. 3. Therefore, the rise time, t_r, in terms of RC time constants is given by (4) and (5).

$$0.2 \cdot T_{pulse} = T_{pulse} \cdot (1 - (\mathrm{e})^{-\frac{t}{RC}}) \qquad (4)$$

and

$$0.6 \cdot T_{pulse} = T_{pulse} \cdot (1 - (\mathrm{e})^{-\frac{t}{RC}}). \qquad (5)$$

So, after solving these two equations independently for $t_{0.2}$ and $t_{0.6}$, the results are $0.22RC$ and $0.92RC$, respectively. Finally, the rise time, t_r, is given by (6).

$$t_r = t_{0.6} - t_{0.2} = 0.92 \cdot RC - 0.22 \cdot RC = 0.7 \cdot RC. \qquad (6)$$

In summary, we have demonstrated and developed a novel RC theory applicable only to solar TEGs. This new theory explicitly shows not only the implications, but also the effects of internal parasitic elements (*R*, *C*, and *L*) on the inner transient heat transfer occurring in any solar energy harvesting TEG. Also, for those who are not very familiar with the *RC* concepts, the t_r found in the current study is the same as t_d found in the conventional *RC* analysis. The only exception made is that, although they both carry significant meaning, they must be interpreted and understood independently.

V. Results and Analysis

This solar TEG energy harvesting system was designed and built to serve typical remote residential areas in developing regions. Real local *DNI* data, the only input to both experimental and the simulated systems, were first recorded by means of a Pyrheliometer and then imported into the Spice model via the built-in piecewise linear (*PWL)* command. Any intermittency in the insolation would automatically be

reflected on the outcome of the model. Hence, as can be seen from Figs. 4 and 5, it is clear that variability remains a big challenge even on the solar TEG energy harvesting systems.

The projected energy harvested, for the benefit of the remote inhabitants, took into consideration not only the actual solar data at the site, but also the typical weather conditions, such as relative humidity, rainfall, and wind speed, etc.

Fig. 4 shows the typical temperature profiles recorded, as well as simulated, for the two sides of the STEG system. These temperatures were plotted separately for clarity purposes, otherwise they would be hard to decipher.

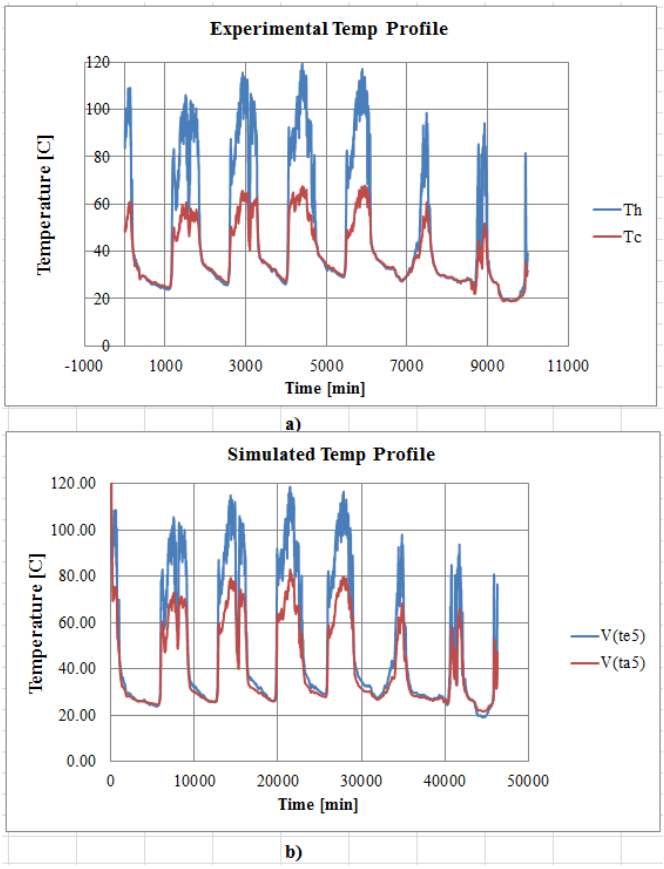

Figure 4 – Temperature variations across the STEG system: a) Experimental temperature profiles, b) Simulated temperature profiles

Consequently, Fig. 4 a) refers to the experimental temperature variations across the energy harvesting system, whereas Fig. 4 b) represents the simulated temperature variations, in which T_H is the same as $V(Te_5)$ and T_C stands for $V(Ta_5)$. As can be seen from these two curves, the error rate between simulation and experiment varied from 0C to about 10C, and more than 80% of it is attributable to the cold side of the STEG system. This acceptable discrepancy between the real-world solar experiment and the LTspice model can be explained by either or both of the followings: 1) the internal parasitic components' variation and 2) the non-homogeneity of the aluminum blocks that were assumed to be pure metal heat exchangers during the computation of the thermal parameters. Another way of viewing this error is that, the LTspice model is roughly 20% less accurate than the actual experiment. This discovery opens room for rectifications in any future similar design.

The voltage supplied by the system is shown in Fig. 5; it varies from 0V (*sunset*) to 8.57V (*clear sunny day*).

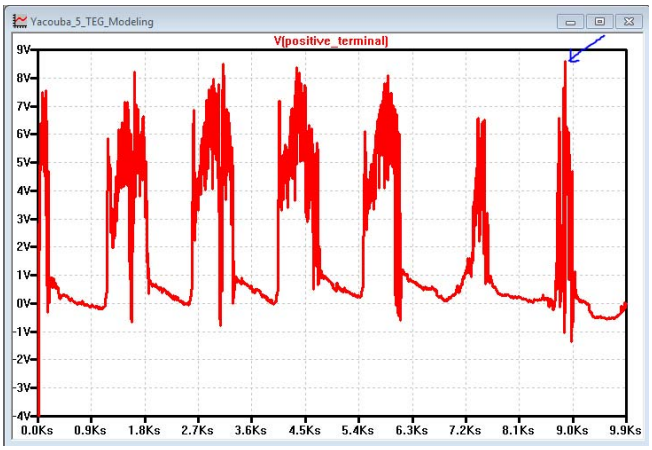

Figure 5 – Weekly output voltage pattern

VI. Conclusion

This paper presented two important analogies: 1) an electrical analogy of a thermal system to simulate a real-world solar thermoelectric generation system and 2) a novel RC analogy to estimate the cold side temperature of a TEG when an impulse of light is applied. Although it is difficult to accurately model the exact behavior of all the physical parts that constitute a real-environment solar energy harvesting system, experimental and simulated results remain in good agreement. This system in conjunction with battery energy storage can be used for all kinds of remote energy applications including telecommunications and bio-sensors.

References

[1] G. W. Crabtree and N. S. Lewis, "Solar energy conversion," *Phys. Today*, vol. 60, no. 3, pp. 37–42, 2007.

[2] P. C. Loh, L. Zhang, S. He, and F. Gao, "Compact integrated solar energy generation systems," *2010 IEEE Energy Convers. Congr. Expo.*, pp. 350–356, 2010.

[3] Y. Moumouni, Y. Baghzouz, and R. F. Boehm, "Power 'smoothing' of a commercial-size photovoltaic system by an energy storage system," in *Proceedings of International Conference on Harmonics and Quality of Power, ICHQP*, 2014.

[4] P. Dziurdzia, "Modeling and simulation of thermoelectric energy harvesting processes," ... *Energy Harvest. Technol. Present* ..., 2011.

[5] M. Cernaianu and A. Cernaianu, "Thermo electrical generator improved model," *Int. Conf. Power* ..., vol. 13, pp. 343–348, 2012.

[6] S. Lineykin and S. Ben-Yaakov, "Modeling and Analysis of Thermoelectric Modules," *IEEE Trans. Ind. Appl.*, vol. 43, no. 2, pp. 505–512, 2007.

[7] C. Alaoui, "Peltier thermoelectric modules modeling and evaluation," *Int. J. Eng.*, no. 5, pp. 114–121, 2011.

[8] A. Mirocha and P. Dziurdzia, "Improved Electrothermal Model of the Thermoe- lectric Generator Implemented in SPICE," pp. 317–320, 2008.

[9] J. Chavez and J. Ortega, "SPICE model of thermoelectric elements including thermal effects," ... , *2000. IMTC 2000.* ..., 2000.

[10] A. Gontean and M. O. Cernaianu, "Parasitic elements modelling in thermoelectric modules," *IET Circuits, Devices Syst.*, vol. 7, no. 4, pp. 177–184, Jul. 2013.

[11] Y. Moumouni and R J. Baker, "Concise Thermal to Electrical Parameters Extraction of Thermoelectric Generator for Spice Modeling," in *IEEE 58th International Midwest Symposi*, 2015.

[12] S. Lineykin and S. Ben-yaakov, "Modeling and Analysis of Thermoelectric Modules," *IEEE Trans. Ind. Electron.*, pp. 2019–2023, 2005.